# Phase-shift analysis of low-energy $\pi^+ p$ data

A. Gashi[a], E. Matsinos[a,y], G.C. Oades[b], G. Rasche[a], and W.S. Woolcock[c]

[a] Institut für Theoretische Physik der Universität,
Winterthurerstrasse 190, CH-8057 Zürich, Switzerland
[b] Institute of Physics, Aarhus University, DK-8000, Aarhus, Denmark
[c] Department of Theoretical Physics, Research School of Physical Sciences and Engineering,
The Australian National University, Canberra ACT 0200, Australia

## Abstract

This work presents the results of a revised analysis of the low-energy (pion laboratory kinetic energy $T_\pi \leq 100$ MeV) $\pi^+ p$ data using recently obtained electromagnetic corrections. The measurements are analyzed assuming extended threshold expansions for the hadronic K-matrix elements. With a few exceptions, the description of the experimental data is satisfactory. Several minimization functions have been used, yielding consistent results. The phase-shift values, obtained in the s and $p_{3/2}$ partial waves, disagree with those of the most recent VPI global-fit solution (SP98); the largest part of this disagreement is removed if we compare our numbers to their single-energy solutions. The s-wave scattering length $a_{0+}$, the p-wave scattering volumes $a_{1+}$ and $a_{1-}$, as well as the hadronic phase shifts themselves, obtained herein, are in agreement with recent work using older electromagnetic corrections; the output of the present work (including meaningful uncertainties) is tabulated in order to enable straightforward use in other applications.

PACS numbers: 11.80.Et, 13.75.Gx, 25.80.Dj

[y] Corresponding author. Present address: The KEY Institute for Brain-Mind Research, University Hospital of Psychiatry, Lenggstrasse 31, CH-8029 Zürich, Switzerland. Electronic mail: evangelos.matsinos@psi.ch, matsinos@key.unizh.ch

# 1 Introduction

There are a number of reasons why the pion-nucleon ( N ) interaction at low energies (pion laboratory kinetic energy T 100 MeV) has recently re-attracted considerable research interest.
a) Experiments, carried out at the meson factories for almost two decades, have yielded an abundance of low-energy data.
b) Chiral-Perturbation Theory ( PT) [1], as a method to draw conclusions from Quantum Chromodynamics (QCD), possesses the potential to interrelate various low-energy hadronic processes [2] and serve as the theoretical basis for the strong interaction in this region.
c) During the last couple of years, clear evidence on the breaking of isospin symmetry in the N system at low energies has been reported in two independent analyses (Refs. [3] and [4]).

A key issue in the interaction of charged hadrons relates to the role the electromagnetic force plays in the particular process; it distorts the 'interesting' part of the interaction, i.e., the hadronic component of the amplitude. To extract the hadronic quantities (i.e., phase shifts, scattering lengths, etc.) from the raw experimental data, one has to apply corrections. The only documented and easy-to-use algorithm, available so far at low energies, has been the NORDITA method [5]. However, there exist three main problems in the NORDITA approach:
a) Their tables extend down to about T = 20 MeV. Recent painstaking experiments on pionic hydrogen [6] and deuterium [7] have directly yielded the 'interaction amplitudes' (scattering lengths) at the N threshold (zero kinetic energy of the interacting partners). The electromagnetic corrections to the 'raw' pionic-hydrogen scattering lengths had to be evaluated in a different scheme [8] (to the NORDITA method). Evidently, a meaningful comparison, between i) the extrapolations of the N amplitudes from the energy corresponding to the scattering data to threshold and ii) the experimentally obtained scattering lengths from pionic hydrogen, necessitates the compatibility of the electromagnetic corrections applied in the two cases; therefore, it is imperative to have a consistent scheme of corrections applicable in the entire low-energy region.
b) Short-range effects were not considered in the NORDITA scheme, a fact which, as the authors of the NORDITA papers explicitly remark in their articles, is 'a serious drawback of the method'.
c) Effects of vacuum polarization were ignored in Ref. [5].
The problem of the modification of the hadronic N amplitudes due to the existence of the electromagnetic interaction has been recently re-assessed. New values for the corrections in the $^{+}$p system are now available [9]; the p electromagnetic corrections will be finalized in the very near future [10].

The present work serves a dual purpose. Firstly, details are given here about the analysis of the low-energy $^{+}$p data leading to the electromagnetic corrections of Ref. [9]. Secondly, the description of the measurements using an extended threshold

expansion of the hadronic K-matrix [11] will be investigated in the light of the recent developments; new hadronic phase shifts will be extracted from the data on the exclusive basis of the low-energy information and with the application of the numerical results of Ref. [9].

## 2 The data base

The low-energy $^+p$ data base comprises 40 experiments [1] with in all 428 data points [13]–[28]; Refs. [13]–[22] correspond to measurements of the differential cross section, Refs. [23] and [24] to measurements of analyzing power, Refs. [25] and [26] to measurements of partial-total cross section, and Refs. [27] and [28] to measurements of total-nuclear cross section. The index and the label, to be used in the following to identify these experiments, as well as some other characteristics, are shown in Table 1. The old measurements of Bertin et al. [13] and of Carter et al. [27] were removed from our data base prior to any analysis; abundant information exists (e.g., see the contributions by G.R. Smith, R.G.E. Timmermans, E. Matsinos, and W.R. Gibbs in Ref. [29]) that either these measurements are erroneous or their (systematic) uncertainties have largely been underestimated. The remaining experiments constitute our starting data base; the statistical approach, pursued in the present work, will suggest the rejection of some additional discrepant data sets on the basis of the individual contributions to the minimization function (see Section 4).

In order to avoid biases in the analysis, the individual contributions to the normalization uncertainty in the measurements of Ref. [19] were combined in quadrature [30].

The statistical analysis in the present article requires the knowledge of both statistical and systematic uncertainties for each experiment. Of course, one may always exclude all experiments in which normalization uncertainties were not given, yet, in order to retain as much information as possible, it was decided that another course should be followed here: these measurements were left in the data base, but were given a lower statistical weight than the complete measurements. To determine the actual weight to be assigned to these data is to some extent arbitrary. We decided to assign a 10 % systematical error to all measurements of differential, partial-total, or total-nuclear cross sections which were <u>not accompanied</u> by a report on the normalization uncertainty; this number is about three times the average normalization uncertainty quoted in meson-factory experiments. It is well known that measurements of the analyzing power are much less affected by normalization uncertainties than differential cross sections (many uncertainties drop out as they

[1] The Bussey et al. data [12] have not been taken into account; unfortunately, these measurements have not appeared in a convenient form which would permit their straightforward inclusion. Given the fact that the low-energy $^+p$ measurements of Ref. [12] comprise only three entries which, additionally, have been taken close to the upper energy limit considered in the present work, these data can neither have any weight in our results nor alter any of our conclusions.

appear both in the nominator and the denominator in the corresponding expressions); the analyzing-power measurements were assigned a 'working' uncertainty of 1 %. Other normalization uncertainties were tried (e.g., 5 % and 15 % for differential, partial-total, or total-nuclear cross sections, 2 % and 5 % for analyzing powers); the changes, thus induced, were found to be insignificant. The assignment of systematic uncertainties applies to 37 data points or 8:6 % of the entire low-energy $^{+}$p data base.

# 3 The optimization problem

Let $n_j$ be the number of the measurements (data points) in the jth data set, and $y_{ij}^{exp}$ and $_{ij}$ denote the measured value and the statistical uncertainty of its ith entry, respectively; let $y_{ij}^{th}$ be the corresponding value estimated on the basis of a parametric model. Allowing the scale change of the data set j, one may introduce the following contribution $_j^2$ (from the jth experiment) to the minimization function:

$$_j^2 = h \left( \frac{z_j \quad 1}{z_j} \right)^{!2} + \sum_{i=1}^{n_j} \left( \frac{z_j y_{ij}^{exp} \quad y_{ij}^{th}}{_{ij}} \right)^{!2} : \qquad (1)$$

The parameter $z_j$ determines the amount by which the jth data set has to be floated in order to match the bulk of the measurements; the parameters $z_j$ should be close to unity for data sets agreeing with the majority of the measurements. The quantity $z_j$ is the uncertainty in the absolute normalization of the jth data set. Evidently, the first term on the right-hand side of Eq. (1) is the penalty one has to pay for floating the absolute normalization of the measurements. Later on, we will comment on the value of $h > 0$ to be chosen; by varying h, one may investigate the sensitivity of the results to the effects of the absolute normalization of the data. The overall minimization function is defined as the sum of all the individual contributions, i.e.,

$$^2 = \sum_{j=1}^{N} \; _j^2 \; ; \qquad (2)$$

where N denotes the number of experiments comprising the data base in the particular run.

The minimization process imposes N conditions to the overall $^2$;

$$\frac{@ \; ^2}{@ z_j} = 0 \quad : \qquad (3)$$

Solving the resulting equations, one may easily deduce the scale factors $z_j$:

$$z_j = \frac{\sum_{i=1}^{n_j} \frac{y_{ij}^{th} y_{ij}^{exp}}{(_{ij})^2} + \frac{h}{(z_j)^2}}{\sum_{i=1}^{n_j} \left( \frac{y_{ij}^{exp}}{_{ij}} \right)^{!2} + \frac{h}{(z_j)^2}} \quad : \qquad (4)$$

Substituting the parameters $z_j$ back to Eq. (1), one finally obtains:

$$\chi^2 = \chi^2_0 \; \frac{\sum_{i=1}^{n_j} \frac{y_{ij}^{exp}(y_{ij}^{exp} - y_{ij}^{th})}{(\delta_{ij})^2}}{\sum_{i=1}^{n_j} \left(\frac{y_{ij}^{exp}}{\delta_{ij}}\right)^2 + \frac{h}{(\delta z_j)^2}} \quad ; \tag{5}$$

where $\chi^2_0$ denotes the sum of the individual contributions

$$\frac{y_{ij}^{exp} - y_{ij}^{th}}{\delta_{ij}}$$

over all data points.

We will now come to a reasonable choice of the parameter $h$. In Ref. [31], $h$ was put equal to the group population $n_j$. One may argue that this choice does not treat the low-$n_j$ and the large-$n_j$ experiments on equal footing; for example, if two experiments, which yielded values of the same physical quantity over the same (or similar) kinematical domain, have very different values of $n_j$, then the principle of economy in the fit dictates that the low-$n_j$ experiment be more susceptible to scale change than the large-$n_j$ one. However, the effect of the absolute normalization is entirely contained in <u>one</u> number for both experiments, i.e., in the normalization uncertainty. In order to inhibit this 'injustice', one may think of the following modifications:
a) Introduce a constant $h$ value for all experiments. For instance, one may use the average number of measurements over the experiments comprising the data base in the particular run ($h = < n >$). A popular choice, which however allows for large 'cheap' (in the sense of the penalty paid) scale changes of the data sets, is $h = 1$.
b) Instead of using the minimization function of Eq. (2), one may choose to minimize the sum of the $\frac{\chi^2_j}{n_j}$ contributions, thus a $\chi^2$ function defined by the formula:

$$\chi^2 = < n > \sum_{j=1}^{N} \frac{\chi^2_j}{n_j} \quad ; \tag{6}$$

where $\chi^2_j$ is given in Eq. (1) with $h = n_j$. It is evident that for 'good' experiments, the ratio $\frac{\chi^2_j}{n_j}$ should be close to unity.

In order to examine the sensitivity of our results to the different treatments of the statistical and systematic uncertainties of the measurements, the following methods have been used in this analysis:
a) Method I: a robust fit described in Ref. [4],
b) Method II: a standard $\chi^2$ fit in which statistical and systematic uncertainties were combined in quadrature,
c) Method III: a $\chi^2$ fit where $\chi^2_j$ is given by Eq. (1) with $h = 1$,

d) Method IV: a $^2$ fit where $^2_j$ is given by Eq. (1) with $h = n_j$,
e) Method V: a $^2$ fit where $^2_j$ is given by Eq. (1) with $h = < n >$, and
f) Method VI: the minimization of the function defined in Eq. (6).
No floating of the data is allowed in methods I and II. We find very little sensitivity of our numerical results to the particular method chosen.

The standard minimization package MINUIT [32] of the CERN library has been used throughout the analysis.

# 4 Investigation of the internal consistency of the data base

Before embarking on the determination of the hadronic quantities from the data, we address the question of the compatibility of the measurements. The expansions of the hadronic K-matrix elements of Ref. [11] have been adopted. For elastic scattering (which is the case for the energy interval considered in the present analysis), the K-matrix formalism connects the hadronic phase shift $^h$ ( ) (for a partial wave defined by the index ) with the corresponding hadronic K-matrix element via the formula:

$$q_c \cot(^h( )) = K^{-1}( ) \quad ; \tag{7}$$

where $q_c$ and denote the pion center-of-mass (c.m.) momentum and kinetic energy, respectively. The $^+p$ interaction proceeds exclusively through the isospin-$\frac{3}{2}$ partial waves. At low energies, only the s and p waves are of importance [2]; thus, only three partial-wave amplitudes are relevant for $^+p$ scattering.

For the s wave, the hadronic K-matrix element may be expanded as:

$$K_{0+}^{-1}( ) = \frac{1}{a} + b \quad + c^2 \quad : \tag{8}$$

For the $p_{1=2}$ wave, a smooth dependence of the hadronic K-matrix element on was assumed:

$$K_1 \quad ( ) = d \quad + e^2 \quad : \tag{9}$$

For the $p_{3=2}$ wave, the existence of the -isobar resonance at = 127 MeV suggests the inclusion of a resonant piece in the hadronic K-matrix; a Breit-Wigner formula with an energy-dependent width [34] has been added on top of the background term described by the sum of a linear and a quadratic term in in the form of Eq. (9). The resonant piece is given by the formula:

$$[K_{1+}( )]_{res} = \frac{m^2}{q^3 \; W} \; \frac{q_c^2}{m^2 \quad W^2} \quad ; \tag{10}$$

[2] The values of the small phase shifts in the d and f partial waves were fixed to the most recent phase-shift solution of the VPI (Virginia Polytechnic Institute) group (SP 98) [33]; this solution gives a slightly better description of the data than all other past solutions.

where  is the width of the resonance at the resonance position, m  stands for the mass of the  -isobar resonance (constant), q  is the pion c.m. momentum at the resonance position, and W  denotes the total c.m. energy of the  $^{+}$p system. Note that the resonant piece $[K_{1+}(\ )]_{res}$ does not introduce any free parameters.

The values of all physical constants have been obtained from Ref. [35].

For a given optimization method (and electromagnetic corrections), a global  t to the  $^{+}$p data was performed.

a) Firstly, the shape of the data sets was checked. For the jth experiment, the ratios

$$r_{ij} = \frac{y_{ij}^{th} \quad y_{ij}^{exp}}{y_{ij}^{exp}} \tag{11}$$

were evaluated for all entries i. This ratio expresses the amount by which the ith entry of the jth experiment has to be scaled in order to meet the bulk of the data. In case that the shape of the jth data set agrees with the trend of the majority of the measurements, the ratio r is expected to be independent of the kinematical variable involved in the particular measurement (i.e., of the scattering angle for di erential cross sections and analyzing powers, or of the energy for partial-total and total-nuclear cross sections); in the case of disagreement in shape, r does not come out constant. A least-squares  t, assuming no dependence (on the kinematical variable involved), was performed to the entries $r_{ij}$ of each individual data set; the individual contributions were weighted with the factor

$$w_{ij} = \frac{1}{(\ r_{ij})^2} \quad ; \tag{12}$$

where $r_{ij}$ denotes the overall uncertainty in $r_{ij}$ (i.e., the statistical uncertainty of the measurement and the 'theoretical' one determined with a robust  t to the data; these two uncertainties were combined in quadrature). The goodness of the  t was investigated in terms of the minimal $^2$ value

$$^2_{min} = \sum_{i=1}^{n_j} w_{ij} r_{ij}^2 \quad \frac{\left[ \sum_{i=1}^{n_j} w_{ij} r_{ij} \right]^2}{\sum_{i=1}^{n_j} w_{ij}} \tag{13}$$

and the corresponding number of degrees of freedom  (i.e., the group population minus one, for the scale factor is determined from the data). The particular data set was termed 'inconsistent', if the constancy of r could be ruled out at the 99 % con dence level. The data set, which could be ruled out at the highest con dence level, was removed from the data base (i.e., one experiment at a time) and the optimization process was repeated until all (remaining) experiments satis ed the acceptance criterion.

b) If an experiment passed the criterion set up at step (a), its normalization was investigated. On the basis of the results of the fit of step (a), an optimal normalization $c_j$ may be obtained via the formula:

$$c_j = \frac{\sum_{i=1}^{n_j} w_{ij} r_{ij}}{\sum_{i=1}^{n_j} w_{ij}} \quad : \tag{14}$$

Its uncertainty is easily obtained from the substitution $^2 = {}^2_{min} + 1$;

$$\sigma_j = \sqrt{\frac{1}{\sum_{i=1}^{n_j} w_{ij}}} \quad : \tag{15}$$

The (generally small) uncertainty $\sigma_j$ was combined in quadrature with the normalization uncertainty $z_j$, quoted in the particular experiment, and the resulting value was compared to the suggested normalization $c_j$ obtained in Eq. (14); as in step (a), a 99 % confidence level was assumed. The data set, which could be ruled out at the highest confidence level, was removed from the data base (again, one experiment at a time) and the optimization process was repeated until all (remaining) experiments satisfied the acceptance criterion.

The procedure, described above, leads to the following conclusions for the $^+p$ data base.

a) The BRACK 90 66:8 MeV data set (entry 25 in Table 1) is by far the most discrepant experiment of the recent data base.

b) The JORAM 95 32:7 MeV data set (entry 28 in Table 1) has a structure which is incompatible with the majority of the measurements.

c) The JORAM 95 44:6 MeV data set (entry 32 in Table 1) has a slope which is absent in the rest of the data.

d) The RITCHIE 83 data (entries 9–12 in Table 1) lie systematically above the bulk of the measurements.

e) The KRISS97 $30^0$ partial-total cross sections (entry 37 in Table 1) are larger than what the bulk of the measurements suggest; though this discrepancy is known for some time, its origin is not yet clear. The two KRISS97 $20^0$ partial-total cross sections (entry 38 in Table 1) were accepted due to their large uncertainties.

f) The FRANK 83 89:6 MeV (entry 16 in Table 1) and the JORAM 95 68:6 MeV (entry 30 in Table 1) data sets have to be removed from the data base on the basis of the results of the analysis with method VI; the former data set lies systematically below the bulk, the latter one above.

The experiments (a)–(c) are rejected due to their shape, whereas (d)–(f) due to their normalization. For the analysts involved in low-energy $N$ physics, the rejection of these data is of no surprise; for example, with the exception of the JORAM 95

44:6 MeV data set, all the above measurements were found incompatible with the bulk of the $^+p$ differential cross sections in Ref. [11].
In the following, the aforementioned measurements (a)–(f) will be excluded from the $^+p$ data base. The 'refined' $^+p$ data base contains 231 entries and comprises 22 experiments. Fits to the data with the methods, listed at the end of Section 3, yielded the coefficients of the hadronic K-matrix elements (e.g., see Eqs. (8) and (9)). The differences between the results of the different methods were found to be small.

# 5 Results and discussion

In detail, the procedure pursued herein is outlined as follows:
a) The electromagnetic corrections were taken from Ref. [9].
b) Fits to the low-energy $^+p$ data were carried out assuming the expansions of the hadronic K-matrix elements as given in Section 4. The hadronic K-matrix elements were corrected (with the values obtained at step (a)), thus leading to the (so-called) nuclear K matrix which was then used to construct the (partial-wave) nuclear amplitudes. Finally, the spin-non-flip and the spin-flip amplitudes were obtained (after the pure Coulomb contributions were added), from which the differential cross sections or analyzing powers were calculated. Fits to the data were carried out with the various minimization methods and the parameters of the model were determined during this optimization process.
c) The values for the various hadronic quantities were obtained via a Monte-Carlo simulation in which the results of the fits of step (b) (i.e., parameter values, errors, and the correlation matrices) were fully taken into account. Averages over the methods of analysis, listed in Section 3, were assumed. All output uncertainties of the fits have been multiplied by the scale factor $\sqrt{\frac{^2}{NDF}}$, where $^2$ denotes the minimal value of the function used in the optimization (not applicable in method I) and NDF is the number of degrees of freedom in the fit.
The above three steps correspond to the final analysis of the data as presented in the present article. For the determination of the electromagnetic corrections of Ref. [9], an iteration was performed. The hadronic phase shifts, obtained in step (c), were used as input for the determination of new electromagnetic corrections (with the model described in Ref. [9]); the cycle was repeated until no changes to the values of the hadronic phase shifts (obtained in the previous iteration) could be seen. In fact, two to three iterations were always sufficient to stabilize the values of the hadronic phase shifts and of the corrections, irrespective of the choice of the phase-shift solution used in order to determine first-step electromagnetic corrections from the experimental data.

We now come to the physics output of this analysis, i.e., to the values the hadronic phase shifts, scattering lengths and volumes as deduced from the low-energy $^+p$ data using the final values of the electromagnetic corrections of Ref. [9].

## 5.1 The parameters

The values of the parameters, achieving the best description of the low-energy $^+p$ data, are displayed in Table 2. They correspond to an average over the methods of analysis listed in Section 3; the sensitivity of the values to the particular method used is very small.

## 5.2 The hadronic phase shifts

Figures 1, 2, and 3 show the energy dependence of the s- and p-wave hadronic phase shifts in the low-energy region in comparison with the SP 98 phase-shift solution [33]. To enable the straightforward application of our results, the corresponding values are listed in Table 3 (including meaningful uncertainties). The values correspond to an average over all the methods of analysis listed in Section 3; the sensitivity of these values to the method used is very small.

Before summarizing our conclusions, drawn on the basis of Figs. 1, 2, and 3, we make some comments about the SP 98 phases. The SP 98 phase-shift solution is a result of a global fit to elastic-scattering data (i.e., up to energies of 2:1 GeV). In such a case, the low-energy data have a very low priority; the energy behaviour of the $N$ amplitudes at low energies is completely determined from the high-energy measurements. Additionally, the SP 98 solution is the outcome of an analysis in which method III has been used in the optimization phase; this method allows for large scale change of the data sets with small penalty. Last but not least, all of the FRANK 83 measurements, amounting to slightly above 1=4 of the low-energy $^+p$ data base, have been floated freely (i.e., no penalty is paid for the scale change of these data).

We now summarize our conclusions:
a) s wave: a big discrepancy with the SP 98 solution is clearly seen; this pronounced difference is due to the strong scale change of the low-energy data in SP 98. It should be emphasized that the largest part of the discrepancy is removed if one compares our values with the SP 98 single-energy solutions.
b) $p_{3=2}$ wave: the low-energy data being taken at face value, a large difference (between our results and the SP 98 phase-shift values) is also seen in this partial wave. This difference is more serious because it suggests modifications in the (so far assumed to be well-known) p-wave part of the $N$ interaction. It should be pointed out once more that this difference is due to the fitting procedure in the SP 98 analysis; within the uncertainties, their single-energy solutions agree with our values.
c) $p_{1=2}$ wave: although the overall status is satisfactory, a small difference (between the two solutions) may be seen close to our upper energy limit.
The present values are in good agreement with the results of Ref. [11]. This is expected because of the large overlap of the data bases used in the two analyses, the similarity of the optimization methods, and the smallness of the electromagnetic

e ects (the NORDITA corrections were used in Ref. [11]).

### 5.3 The scattering lengths and volumes

The s-wave scattering lengths and the p-wave scattering volumes (both denoted by $a$) are defined as:

$$a = \lim_{q_c \to 0} \frac{K(q_c)}{q_c^{2l+1}} \quad ; \tag{16}$$

where $l$ stands for the orbital angular momentum of the $\pi N$ system. Herein, the s-wave scattering length is denoted by $a_{0+}$, whereas the p-wave scattering volumes by $a_{1+}$ and $a_{1-}$.

Our values for the scattering length and volumes are given in Table 4. The values correspond to an average over all the methods of analysis listed in Section 3. The present value of the $a_{0+}$ may be directly compared with the one extracted in Ref. [11] (therein, the s-wave scattering length was denoted by $a_3$) on the basis of the recent differential-cross-section measurements (and different electromagnetic corrections); the agreement is excellent. Good agreement is also seen in the p-wave part of the interaction. At the end of the day, the electromagnetic corrections in the $\pi^+ p$ system are small effects which do not substantially affect the determination of the hadronic component of the interaction.

## 6 Conclusions

This work presents a revised analysis of the low-energy (pion laboratory kinetic energy $T_\pi \leq 100$ MeV) $\pi^+ p$ differential, partial-total, and total-nuclear cross sections, as well as analyzing-power data. The recently obtained electromagnetic corrections of Ref. [9] have been used. The extended threshold expansions of Ref. [11] for the hadronic $K$-matrix elements (in powers of the pion center-of-mass kinetic energy) were assumed; for the description of the resonant $p_{3/2}$ wave, a Breit-Wigner formula with an energy-dependent width has been added on top of the background term.

With a few exceptions (discussed in Section 4 and displayed in Table 1), the description of the experimental data is satisfactory. Several minimization functions have been used (see Section 3) yielding consistent results.

The phase-shift values, obtained in the s and $p_{3/2}$ waves, disagree with those of the most recent VPI solution SP98 [33] (based on a global fit to the experimental data); the largest part of this disagreement is removed if we compare our numbers to their single-energy solutions. This is indicative of the strong scale change of the low-energy experimental data in SP98 in order to achieve compatibility with the information obtained at higher energies.

The scattering length $a_{0+}$, the scattering volumes $a_{1+}$ and $a_{1-}$, as well as the three hadronic phase shifts, obtained here, are in agreement with the corresponding numbers of Ref. [11]. The output of this work (including meaningful uncertainties)

is contained in Tables 2–4 ready for straightforward application.

Acknowledgements. One of us (E. M.) acknowledges a helpful discussion with M. M. Pavan. We thank the Swiss National Foundation and PSI (Paul Scherrer Institut') for financial support.

# References


[1] S. Weinberg, in Chiral Dynamics: Theory and Experiment, Proceedings of the Workshop held at MIT, Cambridge, MA, 1994, edited by A.M. Bernstein and B.R. Holstein (Springer, Berlin, 1995), p. 3; H. Leutwyler, ibid., p. 14.

[2] V. Bernard, N. Kaiser, and Ulf-G. Meissner, Int. J. of Mod. Phys. E 4 2, 193 (1995).

[3] W.R. Gibbs, Li Ai, and W.B. Kaufmann, Phys. Rev. Lett. 74, 3740 (1995).

[4] E. Matsinos, Phys. Rev. C 56, 3014 (1997).

[5] B. Tromborg, S. Waldenstrøm, and I. Øverbø, Phys. Rev. D 15, 725 (1977); Helv. Phys. Acta 51, 584 (1978).

[6] D. Sigg et al., Phys. Rev. Lett. 75, 3245 (1995); D. Sigg et al., Nucl. Phys. A 609, 269 (1996).

[7] D. Chatellard et al., Phys. Rev. Lett. 74, 4157 (1995); also see errata in 75, 3779 (1995); P. Hauser et al., Phys. Rev. C 58, R1869 (1998).

[8] D. Sigg, A. Badertscher, P.F.A. Goudsmit, H.J. Leisi, and G.C. Oades, Nucl. Phys. A 609, 310 (1996).

[9] A. Gashi, E. Matsinos, G.C. Oades, G. Rasche, and W.S. Woolcock, "Electromagnetic corrections to the hadronic phase shifts in $^{+}$p low-energy elastic scattering," ZH-TH Report No. 3/99 (1999).

[10] A. Gashi, E. Matsinos, G.C. Oades, G. Rasche, and W.S. Woolcock, "Electromagnetic corrections for the analysis of p scattering data," in preparation.

[11] N. Fettes and E. Matsinos, Phys. Rev. C 55, 464 (1997).

[12] P.J. Bussey, J.R. Carter, D.R. Dance, D.V. Bugg, A.A. Carter, and A.M. Smith, Nucl. Phys. B 58, 363 (1973).

[13] P.Y. Bertin et al., Nucl. Phys. B 106, 341 (1976).

[14] E.G. Auld et al., Can. J. Phys. 57, 73 (1979).

[15] B.G. Ritchie, R.S. Moore, B.M. Preedom, G. Das, R.C. Minehart, K. Gotow, W.J. Burger, and H.J. Ziock, Phys. Lett. 125B, 128 (1983).

[16] J.S. Frank et al., Phys. Rev. D 28, 1569 (1983).

[17] J.T. Brack et al., Phys. Rev. C 34, 1771 (1986).

[18] J.T. Brack, J.J. Kraushaar, D.J. Rilett, R.A. Ristinen, D.F. Ottewell, G.R. Smith, R.G. Jeppesen, and N.R. Stevenson, Phys. Rev. C 38, 2427 (1988).

[19] U. Wiedner et al., Phys. Rev. D 40, 3568 (1989).

[20] J.T. Brack et al., Phys. Rev. C 41, 2202 (1990).

[21] J.T. Brack et al., Phys. Rev. C 51, 929 (1995).

[22] Ch. Joram et al., Phys. Rev. C 51, 2144 (1995); Ch. Joram et al., ibid. 51, 2159 (1995).

[23] M.E. Sevior et al., Phys. Rev. C 40, 2780 (1989).

[24] R. Wieser et al., Phys. Rev. C 54, 1930 (1996).

[25] E. Friedman (private communication); M.M. Pavan, N Newsletter 11, 117 (1995).

[26] B.J. Kriss et al., N Newsletter 12, 20 (1997).

[27] A.A. Carter, J.R. Williams, D.V. Bugg, P.J. Bussey, and D.R. Dance, Nucl. Phys. B 26, 445 (1971).

[28] E. Pedroni et al., Nucl. Phys. A 300, 321 (1978).

[29] Proceedings of the 7th International Symposium on Meson-Nucleon Physics and the Structure of the Nucleon, Vancouver, B.C. Canada, 1997; N Newsletter 13.

[30] U. Wiedner (private communication).

[31] W. Jaus and W.S. Woolcock, Nucl. Phys. A 608, 389 (1996).

[32] F. James and M. Roos, "MINUIT, Function Minimization and Error Analysis," CERN Report No. D 506 (1987).

[33] R.A. Arndt, R.L. Workman, I.I. Strakovsky, and M.M. Pavan, "N Elastic Scattering Analyses and Dispersion Relation Constraints," nucl-th/9807087; R.A. Arndt and L.D. Roper, SAID on-line program.

[34] T.E.O. Ericson and W. Weise, in Pions and Nuclei, (Clarendon Press, Oxford, 1988), p. 31.

[35] Review of Particle Physics, Particle Data Group, Eur. Phys. J. C 3, 1 (1998).

| Index | Label | T | $n_j$ | Comment |
|---|---|---|---|---|
| 1 | BERTIN76 | 20.8 | 10 | Removed |
| 2 | BERTIN76 | 30.5 | 10 | Removed |
| 3 | BERTIN76 | 39.5 | 10 | Removed |
| 4 | BERTIN76 | 51.5 | 10 | Removed |
| 5 | BERTIN76 | 67.4 | 10 | Removed |
| 6 | BERTIN76 | 81.7 | 10 | Removed |
| 7 | BERTIN76 | 95.9 | 10 | Removed |
| 8 | AULD79 | 47.9 | 11 | |
| 9 | RITCHIE83 | 65.0 | 8 | Rejected |
| 10 | RITCHIE83 | 72.5 | 10 | Rejected |
| 11 | RITCHIE83 | 80.0 | 10 | Rejected |
| 12 | RITCHIE83 | 95.0 | 10 | Rejected |
| 13 | FRANK83 | 29.4 | 28 | |
| 14 | FRANK83 | 49.5 | 28 | |
| 15 | FRANK83 | 69.6 | 27 | |
| 16 | FRANK83 | 89.6 | 27 | Rejected |
| 17 | BRACK86 | 66.8 | 5 | |
| 18 | BRACK86 | 86.8 | 9 | |
| 19 | BRACK86 | 91.7 | 5 | |
| 20 | BRACK86 | 97.9 | 5 | |
| 21 | BRACK88 | 66.8 | 6 | |
| 22 | WIEDNER89 | 54.3 | 19 | |
| 23 | BRACK90 | 30.0 | 6 | |
| 24 | BRACK90 | 45.0 | 8 | |
| 25 | BRACK90 | 66.8 | 11 | Rejected |
| 26 | BRACK95 | 87.1 | 8 | |
| 27 | BRACK95 | 98.1 | 8 | |
| 28 | JORAM95 | 32.7 | 7 | Rejected |
| 29 | JORAM95 | 45.1 | 10 | |
| 30 | JORAM95 | 68.6 | 9 | Rejected |
| 31 | JORAM95 | 32.2 | 20 | |
| 32 | JORAM95 | 44.6 | 20 | Rejected |
| 33 | SEVIOR89 | 98.0 | 6 | |
| 34 | WIESER96 | 68.3 | 7 | |
| Index | Label | $\frac{\min}{L}$ | $n_j$ | Comment |
| 35 | FRIEDMAN95 | 30.0 | 6 | |
| 36 | FRIEDMAN95 | 20.0 | 3 | |
| 37 | KRISS97 | 30.0 | 13 | Rejected |
| 38 | KRISS97 | 20.0 | 2 | |
| 39 | CARTER71 | 0.0 | 2 | Removed |
| 40 | PEDRONI78 | 0.0 | 4 | |

Table 1: The index and the label, used in the present work to identify the $^{+}$p experiments, along with the pion laboratory kinetic energy T (in MeV) for differential cross sections and analyzing power, or the minimal laboratory scattering angle $_{L}^{min}$ (in degrees) for partial-total and total-nuclear cross sections; the number of entries $n_j$ in each experiment is also displayed. If 'Removed' is mentioned in the last column, then the corresponding experiment was removed from the data base prior to any data analysis. If an experiment is termed 'Rejected', then it was removed from the data base during the data analysis on the basis of disagreement with the rest of the data.

| Partial wave | Parameter | Value |
|---|---|---|
| s wave | a | 0:545 0:025 |
| | b | 16:2 3:9 |
| | c | 71 43 |
| $p_{3=2}$ wave | d | 9:41 0:31 |
| | e | 31:2 5:4 |
| $p_{1=2}$ wave | d | 4:75 0:40 |
| | e | 24:6 7:1 |

Table 2: The values of the parameters of the hadronic K-matrix expansion corresponding to the best description of the low-energy $^{+}$p data. a and c are given in GeV $^{1}$, d in GeV $^{2}$, and e in GeV $^{3}$. The values correspond to an average over the methods of analysis listed in Section 3.

| T | $h_{0+}$ | | $h_{1+}$ | | $h_{1-}$ | |
|---|---|---|---|---|---|---|
| 20.0 | 2.35 | 0.05 | 1.25 | 0.01 | 0.25 | 0.02 |
| 25.0 | 2.73 | 0.05 | 1.78 | 0.02 | 0.34 | 0.02 |
| 30.0 | 3.10 | 0.04 | 2.38 | 0.02 | 0.44 | 0.03 |
| 35.0 | 3.46 | 0.04 | 3.07 | 0.02 | 0.54 | 0.03 |
| 40.0 | 3.83 | 0.04 | 3.83 | 0.03 | 0.65 | 0.03 |
| 45.0 | 4.20 | 0.04 | 4.67 | 0.03 | 0.76 | 0.04 |
| 50.0 | 4.57 | 0.05 | 5.60 | 0.03 | 0.87 | 0.04 |
| 55.0 | 4.95 | 0.06 | 6.62 | 0.03 | 0.98 | 0.04 |
| 60.0 | 5.34 | 0.06 | 7.73 | 0.03 | 1.09 | 0.04 |
| 65.0 | 5.72 | 0.07 | 8.95 | 0.03 | 1.20 | 0.04 |
| 70.0 | 6.12 | 0.07 | 10.29 | 0.03 | 1.31 | 0.05 |
| 75.0 | 6.51 | 0.08 | 11.74 | 0.04 | 1.42 | 0.05 |
| 80.0 | 6.91 | 0.08 | 13.33 | 0.04 | 1.52 | 0.06 |
| 85.0 | 7.31 | 0.08 | 15.06 | 0.05 | 1.63 | 0.06 |
| 90.0 | 7.71 | 0.10 | 16.95 | 0.05 | 1.73 | 0.07 |
| 95.0 | 8.11 | 0.13 | 19.01 | 0.06 | 1.83 | 0.09 |
| 100.0 | 8.51 | 0.17 | 21.26 | 0.07 | 1.92 | 0.11 |

**Table 3:** The s- and p-wave hadronic phase shifts (in degrees) extracted from the low-energy $^+p$ data. T (in MeV) denotes the pion laboratory kinetic energy. The values correspond to an average over the methods of analysis listed in Section 3.

| Scattering length | Present value | Value of Ref. [11] |
|---|---|---|
| $a_{0+}$ | $( 76.1 \quad 3.5)10^{-3}$ | $( 77.1 \quad 3.3)10^{-3}$ |
| **Scattering volume** | **Present value** | **Value of Ref. [11]** |
| $a_{1+}$ | $(201.7 \quad 3.0)10^{-3}$ | $(205 \quad 4)10^{-3}$ |
| $a_{1-}$ | $( 46.3 \quad 3.9)10^{-3}$ | $( 46 \quad 7)10^{-3}$ |

**Table 4:** The scattering length (in $_c^{-1}$) and volumes (in $_c^{-3}$) extracted from the low-energy $^+p$ data; $_c$ stands for the mass of the charged pion. The values correspond to an average over the methods of analysis listed in Section 3. The values obtained in Ref. [11] are shown for comparison.

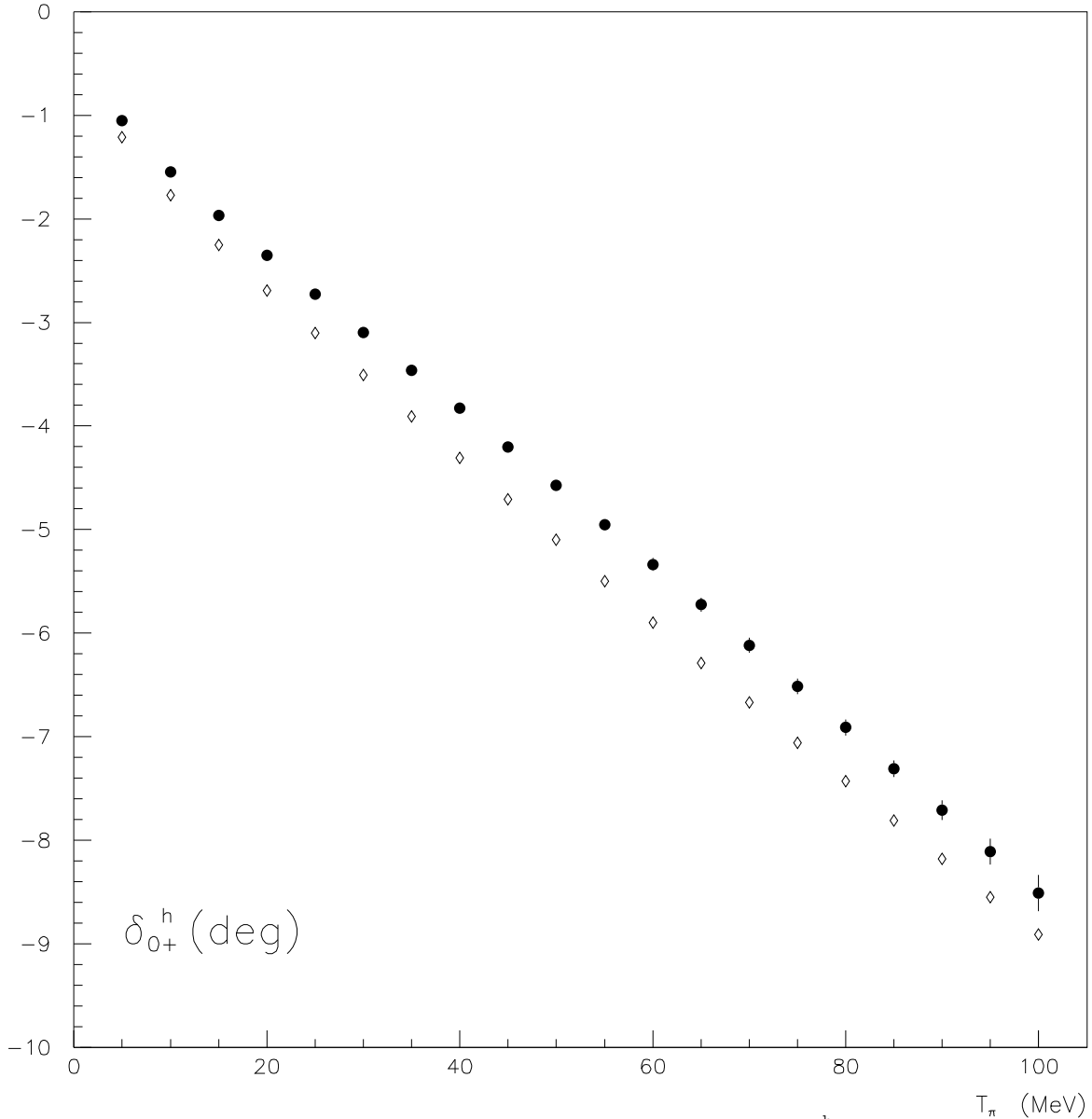


Figure 1: Our values (circles) for the hadronic phase shift $^{h}_{0+}$ (in degrees) extracted from the low-energy $^{+}$p data shown as a function of the pion laboratory kinetic energy T . The diamonds represent the SP 98 phase-shift solution [33]. Our values correspond to an average over the methods of analysis listed in Section 3.

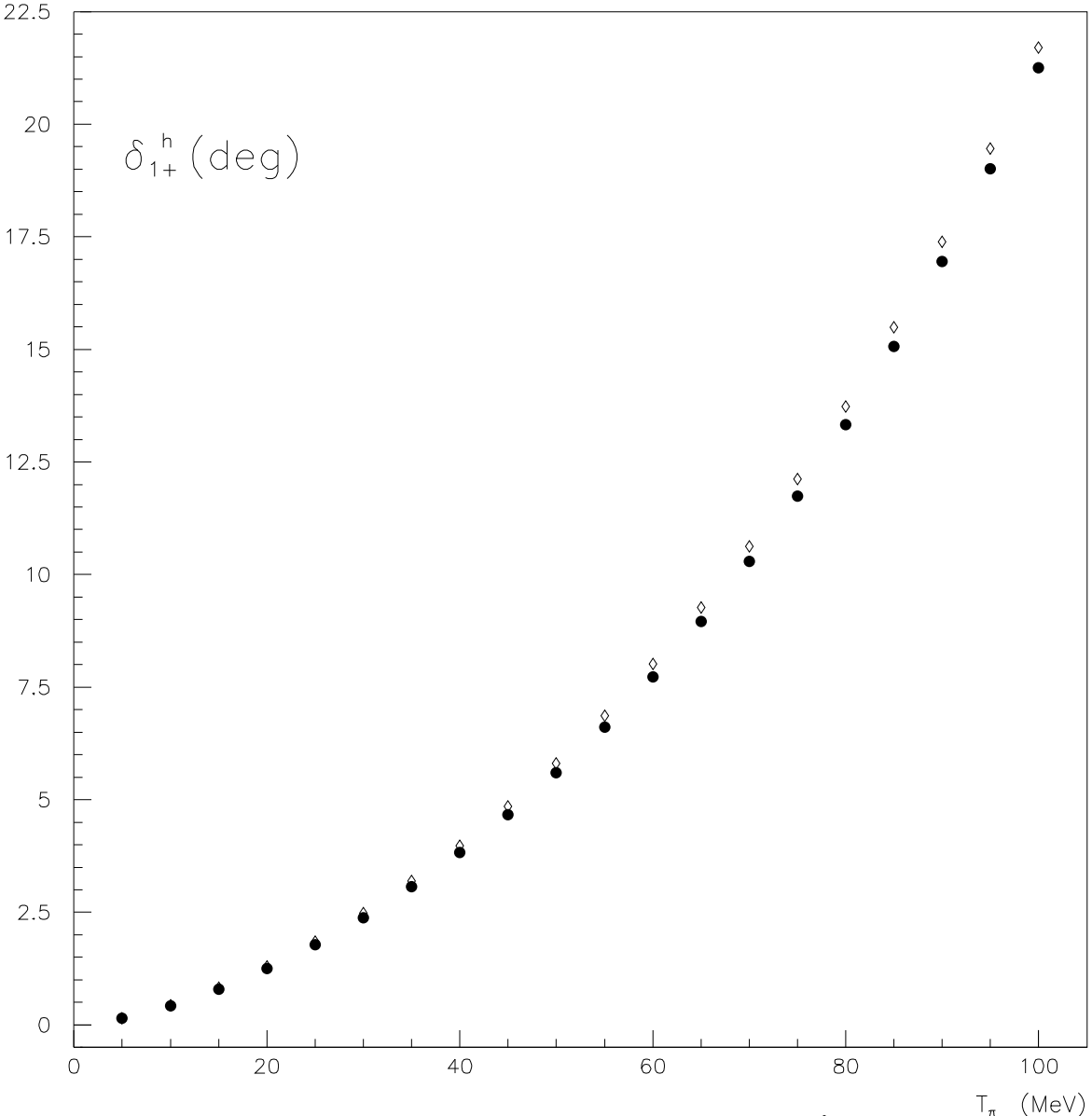


Figure 2: Our values (circles) for the hadronic phase shift $^{h}_{1+}$ (in degrees) extracted from the low-energy $^{+}$p data shown as a function of the pion laboratory kinetic energy T . The diamonds represent the SP 98 phase-shift solution [33]. Our values correspond to an average over the methods of analysis listed in Section 3.

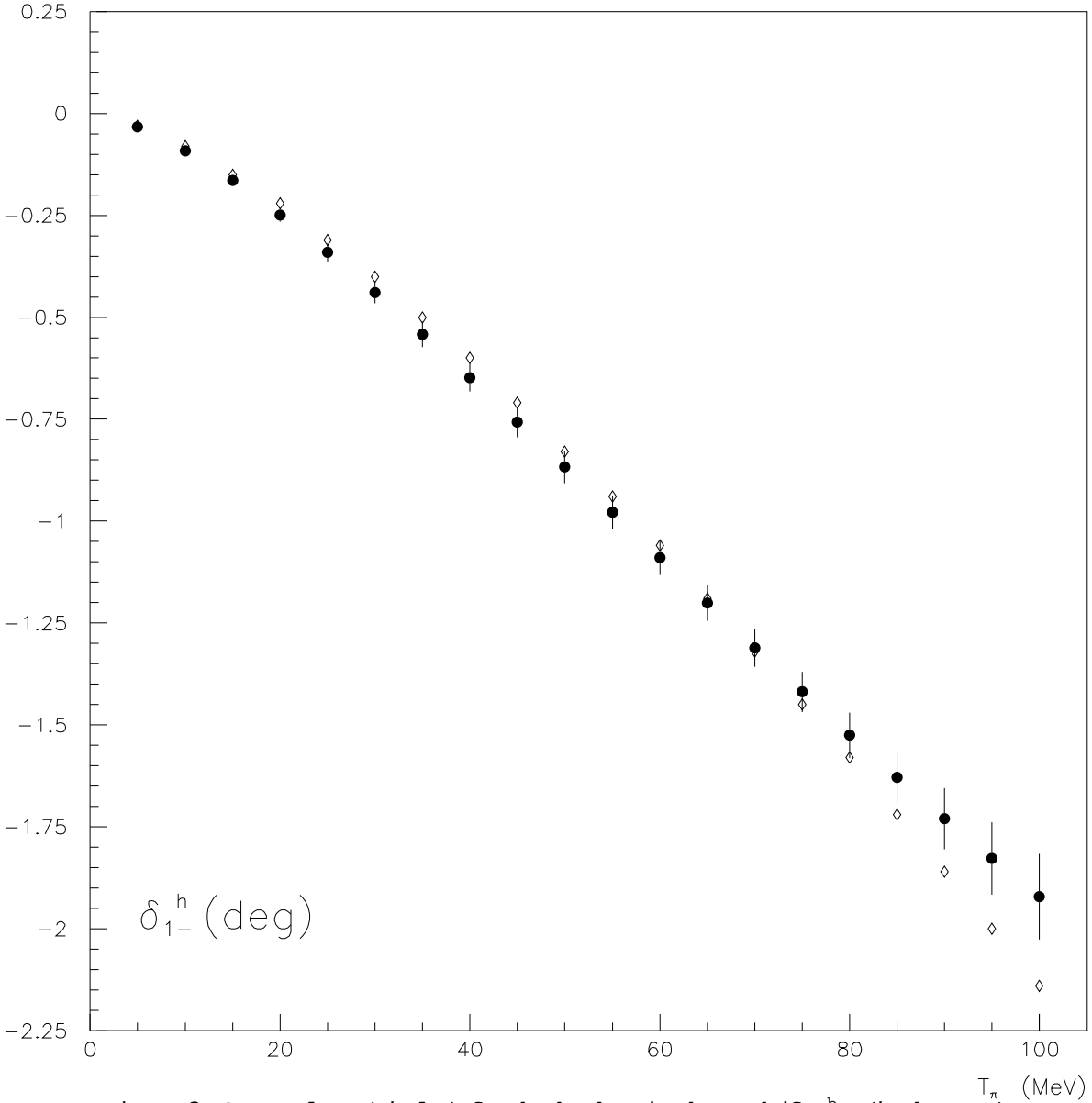


Figure 3: Our values (circles) for the hadronic phase shift $_1^h$ (in degrees) extracted from the low-energy $^+p$ data shown as a function of the pion laboratory kinetic energy T . The diamonds represent the SP 98 phase-shift solution [33]. Our values correspond to an average over the methods of analysis listed in Section 3.